IEEE Photonics Journal
An IEEE Photonics Society Publication

Transmission Analysis of OFDM-Based Wireless Services Over Turbulent Radio-on-FSO Links Modeled by Gamma–Gamma Distribution

Volume 2, Number 3, June 2010

Abdelmoula Bekkali
Chedlia Ben Naila, Student Member, IEEE
Kamugisha Kazaura, Senior Member, IEEE
Kazuhiko Wakamori
Mitsuji Matsumoto, Member, IEEE

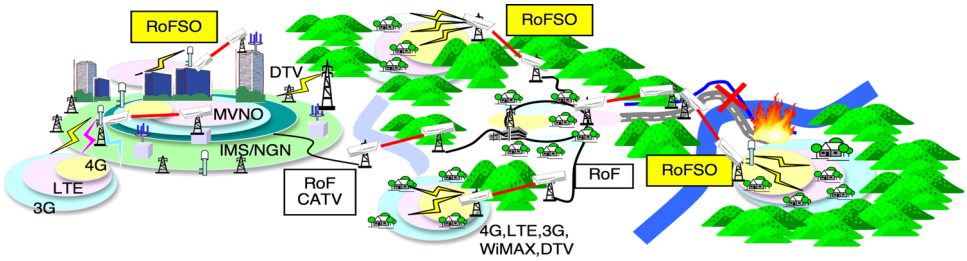

DOI: 10.1109/JPHOT.2010.2050306
1943-0655/$26.00 ©2010 IEEE

Transmission Analysis of OFDM-Based Wireless Services Over Turbulent Radio-on-FSO Links Modeled by Gamma–Gamma Distribution

Abdelmoula Bekkali, Chedlia Ben Naila, *Student Member, IEEE*, Kamugisha Kazaura, *Senior Member, IEEE*, Kazuhiko Wakamori, and Mitsuji Matsumoto, *Member, IEEE*

GITS/GITI Waseda University, Tokyo 169-8050, Japan

DOI: 10.1109/JPHOT.2010.2050306
1943-0655/$26.00 ©2010 IEEE

Manuscript received April 14, 2010; revised May 5, 2010; accepted May 5, 2010. Date of publication May 12, 2010; date of current version June 15, 2010. This work was supported by a Grant-in-aid from the High-tech Research Center Project by the Ministry of Education, Culture, Sports, Science, and Technology, Japan. Corresponding author: A. Bekkali (e-mail: bekkali@fuji.waseda.jp).

Abstract: Radio-on-free space optical (RoFSO) communication systems are rapidly gaining popularity as an efficient and cost-effective means of transferring high data rates and radio frequency (RF) signals with the same capacity as optical fiber. However, the performance of those systems depends strongly on the atmospheric conditions and the nonlinear characteristics of the optical link. In this paper, we introduce an analytical model for the transmission of orthogonal frequency division multiplexing (OFDM)-based signals over free-space optics (FSO) links. Further, we derive a closed-form bit error probability (BEP) and outage probability expressions, taking into account the optical noises, the laser diode nonlinear distortion, and the atmospheric turbulence effect on the FSO channel modeled by the gamma–gamma distribution. This paper reports the most significant parameters that degrade the transmission performance of the OFDM signal over FSO links and indicates the cases that provide the optimal operating conditions for the link. The obtained results can be useful for designing, predicting, and evaluating the RoFSO system's ability to transmit wireless services over turbulent FSO links under actual conditions.

Index Terms: Free-space optics (FSO), orthogonal frequency division multiplexing (OFDM), Radio over Fiber (RoF), radio on FSO, gamma–gamma distribution, atmospheric turbulence.

1. Introduction

The free space optics (FSO) systems are increasingly being considered as a suitable alternative technology for optical fiber networks, especially in areas where the deployment of optical fiber is not feasible and in underserved rural areas lacking broadband network connectivity. The advantages of FSO communications, depending on deployment scenario and application, including ease of deployment, license-free operation, high transmission security, high bit rates, full duplex transmission, and protocol transparency, [1], [2].

At the same time, transmission of radio frequency (RF) signals by means of optical fiber links, which are commonly referred to as radio over fiber (RoF), has been utilized for many years as a cost-effective and high-capacity solution to facilitate the wireless access [3]. However, the applicability of this solution greatly depends on the availability of fiber cable infrastructure and installation costs. In

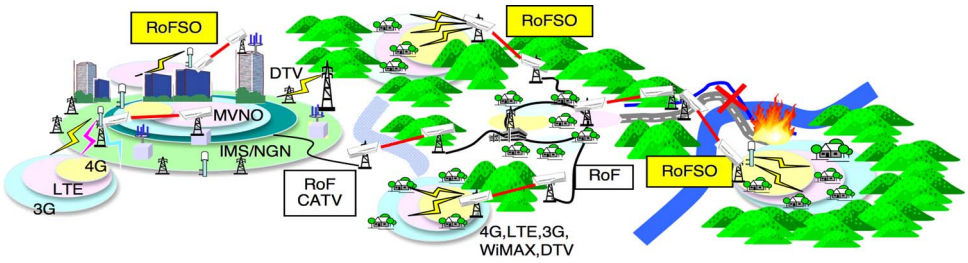

Fig. 1. Scenario depicting deployment of RoFSO links for providing broadband wireless connectivity in urban and rural areas.

the absence of installed fiber cables, FSO links can conveniently be used to transmit RF signals, which are similar to RoF but excluding the fiber medium. Transmission of RF signals using FSO links, which is referred to as radio-on-free space optics (RoFSO), combines the advantages of high transmission capacity enabled by optical device technologies and ease of deployment of wireless links [4], [5]. In terrestrial communications, the RoFSO systems are usually deployed for last-mile access, extending broadband connectivity to underserved areas, and as a fiber back up [6]. However, the performance of RoFSO link can be degraded by many effects, such as fog, rain, atmospheric turbulence, and the non-ideal characteristics of optical transmitters and receivers [4], [7], [8]. Fig. 1 shows the deployment scenario of RoFSO system.

Orthogonal frequency division multiplexing (OFDM) is one of the most popular techniques for broadband wireless communications and is known for its increased robustness against frequency selective fading, narrow-band interference, and high channel efficiency. Consequently, OFDM has been adopted in several high-speed digital communication standards such as digital terrestrial TV broadcasting and the IEEE 802.11 local area network (LAN) and IEEE 802.16 standards. OFDM is also being investigated as a potential candidate for the next-generation mobile wireless systems [9].

The transmission of OFDM over optical link can be considered as special case of multiple-subcarrier modulation (MSM) [10], where multiple independent bit streams are modulated onto subcarriers at different frequencies, multiplexed in the RF domain and transmitted over high capacity optical fiber cables using intensity modulation direct detection (IM/DD) scheme. The MSM signal experiences little distortion and does not need equalization at the receiver end, where each subcarrier can be regarded as a separate narrow-band signal with a lower symbol rate.

The baseband OFDM signal is complex and bipolar, while in IM/DD optical link, a real and positive RF signal is required to drive the laser diode (LD). Therefore, to generate the real OFDM signal, a Hermitian symmetry can be applied to the input vector to the transmitter inverse fast Fourier transform (IFFT) block [11], whereas to transform the OFDM signal to unipolar, a DC bias can be added to the OFDM signal (DC-OFDM) so that the resulting signal becomes positive [12]. The dc bias has to be large enough to prevent clipping and distortion in the optical domain. In general, the main drawbacks of the IM/DD MSM systems are the average optical power inefficiency due to the large added dc bias and distortions due to the LD and optical channel nonlinearity [3], [13]–[15]. This is particularly crucial for IM/DD DC-OFDM, where large number of subcarriers creates unfavorable high peak-to-average power ratios (PAPR) [9], [16], [17]. Moreover, the nonlinearity in the LD causes interference among the subcarriers and a broadening of the overall signal spectrum. These factors introduce a complex situation and pose stringent requirements on the linearity of the optical devices in order to avoid excessive distortion and maintain adequate performance.

In this paper, we investigate the transmission performance of the OFDM signals over a turbulent FSO channel, in terms of the average carrier to noise-plus-distortion ratio (CNDR), bit error probability (BEP), and outage probability. We derive an analytical model for the optimization of the OFDM RoFSO link and the closed-form expressions for BEP and outage probability, taking into account the LD nonlinearity effect and using the gamma–gamma distribution to describe the turbulence-induced fading across weak to strong regimes. In this analysis, we show that the system performance is highly sensitive to the atmospheric turbulence, received optical power, and the

selection of a proper optical modulation index (OMI) for optimum performance. This work provides insight on the system design and performance characteristics relevant in implementing economical links for OFDM-based wireless services transmission, especially in areas lacking fiber infrastructure.

The remainder of this paper is organized as follows. In Section 2, we present the mathematical modeling for the transmission of OFDM signals over turbulent RoFSO link. The analytical results are shown and discussed in Section 3. Finally, Section 4 concludes the paper.

2. System Model

2.1. FSO Channel Characteristics

In FSO channel, the atmospheric turbulence causes irradiance fluctuations, known as scintillation, on the received signals propagating along a horizontal path near ground. Scintillation is mainly caused by small temperature variations in the atmosphere, resulting in refraction-index random variations. Different statistical models have been proposed over the years to describe the atmospheric turbulence channels for varying degrees of strength [18]. For weak turbulence regime, the probability density function (PDF) of the intensity fluctuation is modeled as lognormal distribution, whereas for moderate to strong regimes, the gamma–gamma distribution is used.

The gamma–gamma model describes both small-scale and large-scale atmospheric fluctuations and factorizes the irradiance as the product of two independent random processes, each having a gamma PDF, and defined as [18]

$$p_X(x) = \frac{2(\alpha\beta)^{\frac{\alpha+\beta}{2}}}{\Gamma(\alpha)\Gamma(\beta)} x^{\frac{\alpha+\beta}{2}-1} K_{\alpha-\beta}(2\sqrt{\alpha\beta x}), \quad x > 0 \tag{1}$$

where $\Gamma(\cdot)$ is the Gamma function, $K_n(\cdot)$ is the modified Bessel function of the second kind of order n, α and β are the effective numbers of small scale and large scale eddies of the scattering environment and defined for spherical wave with aperture-averaged scintillation as

$$\alpha = \left[\exp\left\{\frac{0.49\sigma^2}{(1+0.18d^2+0.56\sigma^{12/5})^{7/6}}\right\} - 1\right]^{-1} \tag{2a}$$

$$\beta = \left[\exp\left\{\frac{0.51\sigma^2(1+0.69\sigma^{12/5})^{-5/6}}{1+0.9d^2+0.62d^2\sigma^{12/5}}\right\} - 1\right]^{-1} \tag{2b}$$

where $\sigma^2 = 0.5C_n^2k^{7/6}L^{11/6}$ and $d = \sqrt{(\pi D^2/2\lambda L)}$, $D(m)$ is the diameter of the receiver collecting lens aperture, $\lambda(m)$ is the wavelength, $L(m)$ is the link distance, and $C_n^2(m^{-2/3})$ is the refractive index structure parameter. The scintillation index $S.I$ can be expressed in term of α and β as follows [18]:

$$S.I = \frac{1}{\alpha} + \frac{1}{\beta} + \frac{1}{\alpha\beta}. \tag{3}$$

The gamma–gamma distribution is a more general model, which includes the results of the K-distribution model (i.e., when $\beta = 1$).

2.2. OFDM Signal Transmission Over RoFSO Link

OFDM is a kind of multicarrier transmission in which high data rate streams are split into lower rate streams and then transmitted simultaneously over several narrow-band subcarriers. The subcarriers are themselves modulated by using phase shift keying (PSK) or quadrature amplitude modulation (QAM) and are then carried on a high frequency carrier. OFDM can be simply defined as a form of multicarrier modulation where its carrier spacing is carefully selected so that each subcarrier is orthogonal to the other subcarriers and can be separated at the receiver by correlation techniques; hence, intersymbol interference among channels can be eliminated. The set of orthogonal carriers is realized by using the inverse fast Fourier transform (IFFT) at the transmitter

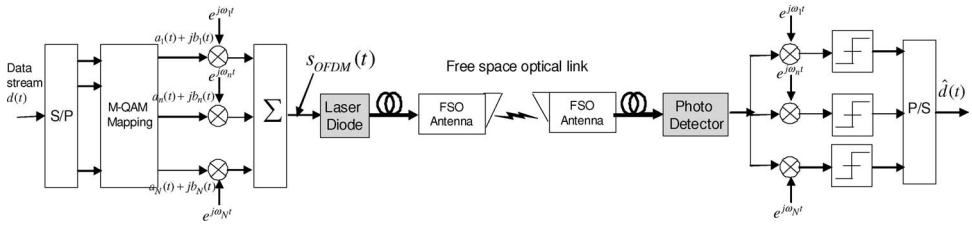

Fig. 2. Basic configuration of OFDM signal transmission over FSO link.

and the fast Fourier transform (FFT) at the receiver and requires no equalization [9]. The basic configuration of OFDM signal transmission over FSO link is shown in Fig. 2.

The OFDM signal for N subcarriers, after up-conversion to the wireless service carrier frequency f_c, can be written as

$$s_{\mathrm{OFDM}}(t) = \sum_{n=0}^{N-1} s_n(t) = \sum_{n=0}^{N-1} X_n \exp(j(\omega_n + 2\pi f_c)t), \quad 0 \le t < T_s \tag{4}$$

where $\{\omega_n = (2\pi n/T_s), n = 0, 1, \ldots, N-1\}$ are the set of orthogonal subcarriers frequency, T_s is the OFDM symbol duration, and $X_n = a_n + jb_n$ is the complex data symbol in the nth subcarrier, with a_n and b_n the in-phase and quadrature modulation symbols, respectively. The first raw data is mapped according to different types of modulation techniques (QPSK, 16QAM, 64QAM), depending upon data rate. Each symbol X_n is amplitude modulated on orthogonal subcarriers. This process is performed using the IFFT which guarantees that all the subcarriers are orthogonal to each other over the symbol interval [9], [12]. Here, we set the guard interval to zero and thus the OFDM symbol duration T_s equals to the Fourier analysis window. The $s_{\mathrm{OFDM}}(t)$ is real by enforcing the conjugate-symmetry (Hermitian symmetry) of the IFFT input vector, i.e., $X_{N-k} = X_k^*$, $k = 1, \ldots, N/2$, The first input X_0, corresponding to the zero frequency, needs to be real-valued and is generally left unmodulated. In general, the need for Hermitian symmetry at the input requires doubling the size of the IFFT block N_{FFT} by extending the symbols $\{X_k, k = 0, 1, \ldots, N-1\}$ with zeros to the length $N_{\mathrm{FFT}} = 2N$. This approach with real-valued IFFT output is used in digital subscriber line (DSL) systems and is known as discrete multitone (DMT) [11]. Due to frequency selectivity, the subcarriers experience in general different channel gains which can be mitigated through the use of many narrow subcarriers.

The signal $s_{\mathrm{OFDM}}(t)$ is then used to modulate the optical intensity of LD to be transmitted through fiber optics. The LD nonlinearity causes mixing of users signals, resulting in generation of harmonics and inter-modulation distortions (IMD). The optical power output from the LD is proportional to the modulating signals as [3]

$$P(t) = P_t \left(1 + \sum_{n=0}^{N-1} m_n s_n(t) + a_3 \left[\sum_{n=0}^{N-1} m_n s_n(t) \right]^3 \right) \tag{5}$$

where P_t is the average transmitted optical power, a_3 is the third order nonlinearity coefficient, and m_n is the OMI for each subcarrier, where the total OMI m_{Total} is given by

$$m_{\mathrm{Total}} = \frac{1}{N} \sqrt{\sum_{n=0}^{N-1} m_n^2}. \tag{6}$$

We assume that the field at any point in the FSO link can be written as the product of the free-space field attenuation factors and the stochastic amplitude to describe the field perturbation. The

received optical power at the photo detector (PD) input can be mathematically described as follows:

$$P_{r,\mathrm{FSO}}(t) = P(t) L_{\alpha} L_{\mathrm{Scint}} L_{\mathrm{Atm}} X + n_{\mathrm{FSO}}(t) \tag{7}$$

where $P(t)$ is the output power from the LD that is transmitted over free space using FSO antenna, L_{Scint} is the loss due to the atmospheric turbulence, L_{Atm} is the loss due to the atmosphere, including rain and low-visibility attenuation losses, and L_{α} is the loss which includes optical fiber loss, FSO geometrical loss, and FSO pointing error loss. $n_{\mathrm{FSO}}(t)$ characterizes the additive white Gaussian noise (AWGN), and X quantifies the variation of the signal fading due to atmospheric turbulence transmission effects and its PDF $p_X(x)$ defined by (1).

Finally, substituting (5) into (7), and assuming that the FSO noise can be filtered in the PD, the output current of the PD can be expressed as follows:

$$i(t, X) = I_{\mathrm{ph}} \left(1 + \sum_{n=0}^{N-1} m_n s_n(t) + a_3 \left[\sum_{n=0}^{N-1} m_n s_n(t) \right]^3 \right) + n_{\mathrm{opt}}(t) \tag{8}$$

$$I_{\mathrm{ph}} = \rho L_{\alpha} L_{\mathrm{Scint}} L_{\mathrm{Atm}} P_t X \tag{9}$$

where I_{ph} is the dc of the received photocurrent $i(t, X)$, ρ is the responsivity of the PD, and $n_{\mathrm{opt}}(t)$ is the AWGN with a double-sided power spectral density (PSD) of $N_0/2$. The Gaussian noise models the noise processes in the RoF link, which is the sum of thermal noise, shot noise, and relative intensity noise (RIN) processes. The shot noise is a function of the mean optical power; the RIN is a function of the square of the optical power, while the thermal noise is signal independent. The total noise power is defined as [3]

$$N_0 = \frac{4 K_B T_{\mathrm{abs}} F}{R_L} + 2 q I_{\mathrm{ph}} + (\mathrm{RIN}) I_{\mathrm{ph}}^2 \tag{10}$$

where K_B is the Boltzmann's constant, T_{abs} is the absolute temperature, F is the noise figure of the receiver electronics, R_L is the PD load resistor, and q is the electron charge. Note that, the received photocurrent I_{ph} is proportional to X and consequently has the same statistic.

2.3. CNDR Analysis

For the sake of simplicity, we assume all the tones to be modulated with the same modulation index m_n. Hence, according to (6), the OMI per subcarrier m_n is derived as

$$m_n = \frac{m_{\mathrm{Total}}}{\sqrt{N}}, \quad n = 0, 1, \ldots, N-1. \tag{11}$$

The desired signal power with respect to subcarrier frequency ω_n can be expressed as

$$C = \frac{1}{2} m^2 I_{\mathrm{ph}}^2. \tag{12}$$

The third order intermodulation distortion (IMD3) which falls into carrier ω_n among equally spaced N carriers can be described as [3]

$$\sigma_{\mathrm{IMD}}^2 = \frac{1}{2} \left(\frac{3}{4} a_3 m_n^3 D_2(N, n) + \frac{3}{2} a_3 m_n^3 D_3(N, n) \right)^2 I_{\mathrm{ph}}^2 \tag{13}$$

where $D_2(N, n)$ and $D_3(N, n)$ represent the number of intermodulation distortion products which influence the desired carrier and are given by [3]

$$D_2(N, n) = \frac{1}{2} \left(N - 2 - \frac{1}{2} \left(1 - (-1)^N \right) (-1)^n \right) \tag{14a}$$

$$D_3(N, n) = \frac{n}{2} (N - n + 1) + \frac{1}{4} \left((N-3)^2 - 5 \right) - \frac{1}{8} \left(1 - (-1)^N \right) (-1)^{N+n}. \tag{14b}$$

Therefore, the received CNDR per subcarrier CNDR_n with scintillation can be defined statistically as a function of the expected desired signal power C, the third-order intermodulation distortion power σ^2_{IMD}, and the optical noise power per subcarrier N_0/T_s, that is

$$\mathrm{CNDR}_n(X) = \frac{C}{\frac{N_0}{T_s} + \sigma^2_{\mathrm{IMD}}}. \tag{15}$$

The optical modulation index helps us to determine the best CNDR for better performance of the system. The optimum optical modulation index per subcarrier $m_{\mathrm{opt},n}$ of the laser transmitter which results in maximum CNDR can be obtained by differentiating (15), with respect to m_n and is given by

$$m_{\mathrm{opt},n} = \left(\frac{N_0/T_s}{\left(\frac{3}{4} a_3 D_2(N,n) + \frac{3}{2} a_3 D_3(N,n)\right)^2 I^2_{\mathrm{ph}}} \right)^{\frac{1}{6}}. \tag{16}$$

Hence, using (11), the total optimal OMI m_{opt} of the system yields

$$m_{\mathrm{opt}} = \sqrt{N} \times \left(\frac{N_0/T_s}{\left(\frac{3}{4} a_3 D_2(N,n) + \frac{3}{2} a_3 D_3(N,n)\right)^2 I^2_{\mathrm{ph}}} \right)^{\frac{1}{6}}. \tag{17}$$

2.4. Symbol and Bit Error Probability Analysis

In this subsection, we analyze the performance of OFDM systems with M-QAM modulation. It is important to determine the degree to which the FSO link carrying OFDM signals may be expected to be degraded due to the atmospheric turbulence, by computing the symbol error probability (SEP) P_s and BEP P_b. We assume that the intermodulation distortion noise is Gaussian distributed so that the total noise defined in (15) is Gaussian. The SEP per subcarrier $P_{s,n}$ for the received M-QAM-OFDM signal, where $M = 2^k$ and k is an even number, is given by [19]

$$P_{s,n}(X) = 2(1 - \sqrt{M}^{-1})\,\mathrm{erfc}\left(\sqrt{A \times \mathrm{CNDR}_n(X)}\right) \tag{18}$$

where $A = 3/[2(M-1)]$, $\mathrm{erfc}(\cdot)$ is the complementary error function.

Using (15), the average $P_{s,n}$ can be obtained by averaging (18) over the scintillation distribution

$$\begin{aligned}\langle P_{s,n}\rangle &= 2(1 - \sqrt{M}^{-1}) \int_0^\infty \mathrm{erfc}\left(\sqrt{\frac{AC}{\sigma^2_N + \sigma^2_{\mathrm{IMD}}}}\right) p_X(x)\,dx \\ &= 2(1 - \sqrt{M}^{-1}) \frac{2(\alpha\beta)^{\frac{\alpha+\beta}{2}}}{\Gamma(\alpha)\Gamma(\beta)} \int_0^\infty \mathrm{erfc}\left(\sqrt{\frac{AC}{\sigma^2_N + \sigma^2_{\mathrm{IMD}}}}\right) x^{\frac{\alpha+\beta}{2}-1} K_{\alpha-\beta}(2\sqrt{\alpha\beta x})\,dx \end{aligned} \tag{19}$$

where $P_{r,0} = L_\alpha L_{\mathrm{Atm}} P_t$ is the received optical power in the absence of turbulence.

In order to solve the integral of (19), we assume that the CNDR can be approximated by averaging the noises and the intermodulation distortion over scintillation, i.e., $\mathrm{CNDR}_n(X) \approx C/(\langle\sigma^2_N\rangle + \langle\sigma^2_{\mathrm{IMD}}\rangle)$, where $\langle . \rangle$ denotes the average over scintillation. Note that the denominator is a second order polynomial with the scintillation x as variable. Hence, we use the expressions $\mathrm{erfc}(\sqrt{z}) = (1/\sqrt{\pi}) G^{2,0}_{1,2}[z|^{1}_{0,1/2}]$ [20, Eq. 06.27.26.0006.01] and $K_n(z) = (1/2) G^{2,0}_{0,2}[z^2/4|_{n/2,-n/2}]$ [20, Eq. 03. 04. 26.0008.01], where $G^{a,b}_{c,d}(\cdot)$ is a MeijerG function, which is a standard built-in function in most well-known mathematical software packages such as Mathematica and Maple. Moreover, the MeijerG function can be written in terms of the more familiar generalized hypergeometric functions [20], [21]. Equation (19) can be rewritten as

$$\langle P_{s,n}\rangle = \frac{(1 - \sqrt{M}^{-1})(\alpha\beta)^{\frac{\alpha+\beta}{2}}}{\sqrt{\pi}\Gamma(\alpha)\Gamma(\beta)} \int_0^\infty G^{2,0}_{1,2}\left(\frac{\frac{1}{2} A (m_n \rho P_{r,0})^2 x^2}{\langle\sigma^2_N\rangle + \langle\sigma^2_{\mathrm{IMD}}\rangle} \Bigg|^{1}_{0,\frac{1}{2}} \right) x^{\frac{\alpha+\beta}{2}-1} G^{2,0}_{0,2}\left(\alpha\beta x|_{\frac{\alpha-\beta}{2},\frac{\beta-\alpha}{2}}\right) dx. \tag{20}$$

Finally, a closed-form expression of the average SEP per subcarrier $\langle P_{s,n}\rangle$ is then derived using [20, Eq. 07.34.21. 0013.01]

$$\langle P_{s,n}\rangle = (1-\sqrt{M}^{-1})\frac{2^{\alpha+\beta-1}}{\pi\sqrt{\pi}\Gamma(\alpha)\Gamma(\beta)}\ G_{5,2}^{2,4}\left(\frac{2^3A(m_n\rho P_{r,0})^2}{(\langle\sigma_N^2\rangle+\langle\sigma_{\text{IMD}}^2\rangle)(\alpha\beta)^2}\middle|\begin{matrix}\frac{1-\alpha}{2},\frac{2-\alpha}{2},\frac{1-\beta}{2},\frac{2-\beta}{2},1\\ \\ 0,\frac{1}{2}\end{matrix}\right). \tag{21}$$

Assuming that the Gray-coded mapping is used at the transmitter, the average BEP per subcarrier $\langle P_{b,n}\rangle$ can be obtained from (21) as

$$\langle P_{b,n}\rangle = \frac{1}{\text{Log}_2(M)}\langle P_{s,n}\rangle. \tag{22}$$

When the number of subcarriers is large, the total average bit error probability $\langle P_b\rangle$ over the entire OFDM band can be derived based on law of large numbers (LLN)

$$\langle P_b\rangle = \frac{1}{N}\sum_{n=0}^{N-1}\langle P_{b,n}\rangle. \tag{23}$$

2.5. Outage Probability Analysis

The outage probability is a commonly used performance metric in fading channels. It is defined as the probability that the instantaneous CNDR falls below a specified threshold CNDR_{th}, which represents a specified value of the CNDR above which the quality of the channel is satisfactory. It is a useful metric to characterize the effect of the atmospheric turbulence on the CNDR and, thus, on the BEP P_b. The outage probability per subcarrier $P_{\text{Out},n}$ is defined as follows:

$$P_{\text{Out},n}(\text{CNDR}_{\text{th}}) = \Pr(\text{CNDR}_n < \text{CNDR}_{\text{th}}). \tag{24}$$

If we define a constant I_{th} as a ratio $I_{\text{th}} = (\sqrt{2\text{CNDR}_{\text{th}}(\langle\sigma_N^2\rangle+\langle\sigma_{\text{IMD}}^2\rangle)}/\rho m P_{r,0})$, (24) can be rewritten as

$$\begin{aligned} P_{\text{Out},n}(\text{CNDR}_{\text{th}}) &= \int_0^{I_{\text{th}}} p_X(x)\,dx \\ &= \int_0^{I_{\text{th}}} \frac{2(\alpha\beta)^{\frac{\alpha+\beta}{2}}}{\Gamma(\alpha)\Gamma(\beta)}x^{\frac{\alpha+\beta}{2}-1}K_{\alpha-\beta}(2\sqrt{\alpha\beta x})\,dx. \end{aligned} \tag{25}$$

Using the equations [21, Eq. 6.592.2] and [20, Eq. 03.04.26.0008.01], a closed-form expression of the outage probability per subcarrier $P_{\text{Out},n}$ yields

$$P_{\text{Out},n}(\text{CNDR}_{\text{th}}) = \frac{(\alpha\beta)^{\frac{\alpha+\beta}{2}}}{\Gamma(\alpha)\Gamma(\beta)}I_{\text{th}}\ G_{1,3}^{2,1}\left(\alpha\beta I_{\text{th}}\middle|\begin{matrix}1-\frac{\alpha-\beta}{2}\\ \frac{\alpha-\beta}{2},\frac{\beta-\alpha}{2},\frac{\alpha+\beta}{2}\end{matrix}\right). \tag{26}$$

Similar to the total average BEP, the resulting total outage probability P_{Out} of the system can be expressed as

$$P_{\text{Out}}(\text{CNDR}_{\text{th}}) = \frac{1}{N}\sum_{n=0}^{N-1}P_{\text{Out},n}(\text{CNDR}_{\text{th}}) \tag{27}$$

3. Results and Discussion

In this paper, we select the integrated services digital broadcasting-terrestrial (ISDB-T) signal standard [22] in order to evaluate the degradation of an OFDM-based wireless service transmission

TABLE 1

ISDB-T signal transmission parameters

Parameter	Value
Carrier frequency (f_c)	473.14 MHz
Number of carriers (N)	5617 (Mode 3)
OFDM Symbol duration (T_s)	1008 μs
Operating wavelength (λ)	1551.72 nm
LD Output power	5.8dBm
Transmitted optical power (P_t)	20dBm
Detector responsivity (ρ)	0.8 A/W
Relative intensity noise (RIN)	-130dB/Hz
Absolute temperature (T_{abs})	300K
PD load resistor (R_L)	50 Ω
Third order IMD (a_3)	9 $\times 10^{-4}$

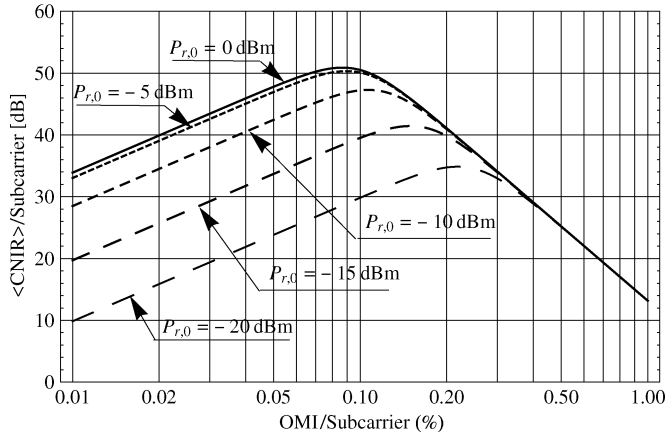

Fig. 3. Variation of the CNDR per subcarrier with the OMI per subcarrier for different values of the received optical power.

over FSO link affected by the atmospheric turbulence and optical nonlinear distortion. Numerical results of the received CNDR, BEP, and outage probability are generated and studied based on (15), (23), and (27), respectively. Throughout this study, the BEP is analyzed without using the forward error correction (FEC) coding technique. In general, the ISDB-T standard uses concatenated codes as error-correction schemes, namely, Reed–Solomon (204, 188) code for the outer code and a convolutional code for the inner code [22]. The values of all parameters used in the numerical calculation are given in Table 1.

Before presenting the numerical results, we define the average of CNDR over the atmospheric turbulence random process X as $\langle \text{CNDR} \rangle = \int_0^\infty \text{CNDR}(m, x) p_X(x) dx$.

Fig. 3 plots the variation of the average received ISDB-T CNDR per subcarrier $\langle \text{CNDR}_n \rangle$ predicted from (15) with respect to the OMI per subcarrier m_n for different values of the received optical power in the absence of turbulence $P_{r,0} = \{-25 \text{ dBm}, -20 \text{ dBm}, -15 \text{ dBm}, -10 \text{ dBm}, -5 \text{ dBm}\}$ and with scintillation parameters $(\alpha, \beta) = (4, 1)$. From the figure, it can be observed that the value of CNDR clearly depends on the OMI m_n. For instance, when $P_{r,0} = -5$ dBm, the CNDR value improves as the OMI value is increased from $m_n = 0\%$ to 0.1% but deteriorates as the OMI value is increasing from $m_n = 0.1\%$ to 100%. The maximum CNDR value is approximately 52 dB, and is achieved at $m_n = 0.1\%$. This can be explained as follows: When m_n is small, the received carrier power is low, and the intermodulation distortion is negligible; thus, the optical noise $\langle \sigma_N^2 \rangle$ dominates, and the CNDR can be approximated as $\langle \text{CNDR}_n \rangle \approx C / \langle \sigma_N^2 \rangle$. As shown in the previous section, there are three main noise sources: the RIN of the LD, the shot noise, and the thermal noise. Among them, the thermal noise affects the CNDR performance when the received optical power is small, whereas when m_n is large, the intermodulation distortion $\langle \sigma_{\text{IMD}}^2 \rangle$ dominates, and in this case, the

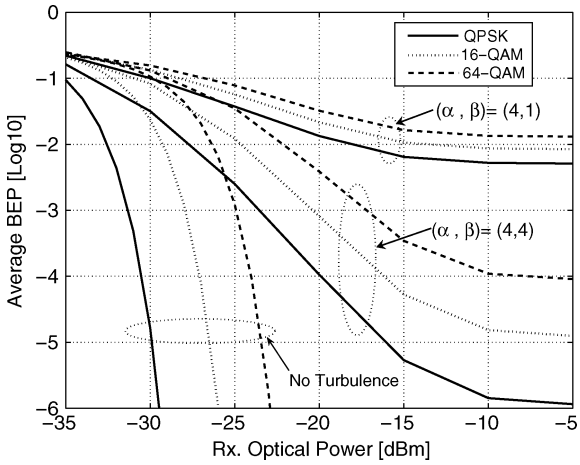

Fig. 4. Variation of the average BEP for QPSK, 16-QAM, and 64-QAM with the received optical power.

CNDR is approximated as $\langle \text{CNDR}_n \rangle \approx C/\langle \sigma^2_{\text{IMD}} \rangle$. Therefore, specifying an appropriate and optimal value of the OMI m_{opt} is essential in optimizing the system performance. The optimal OMI $m_{\text{opt},n}$ that leads to the optimal value of the CNDR per subcarrier $\langle \text{CNDR}_{\text{opt},n} \rangle$ and is given by (16) helps us to determine the best CNDR for better performance of the system. Furthermore, we observe that the $\langle \text{CNDR}_n \rangle$ degrades with the increase of the received optical power. As a result, the pair $(m_{\text{opt},n}, \langle \text{CNDR}_{\text{opt},n} \rangle)$ can take different values with the variation of the received optical power. For example, for $P_{r,0} = -5$ dBm, the optimal CNDR is about $\langle \text{CNIR}_{\text{opt},n} \rangle = 50$ dB at $m_{\text{opt},n} = 0.09\%$, whereas with the same value of m_n, the $\langle \text{CNDR}_n \rangle = 29$ dB for $P_{r,0} = -25$ dBm. However, for $P_{r,0} = -25$ dBm, the optimal CNDR is about $\langle \text{CNIR}_{\text{opt},n} \rangle = 35$ dB at $m_{\text{opt},n} = 0.2\%$, which leads to a CNIR penalty equal to 6 dB. These results indicate the importance of the optical link carrying RF signals and demonstrate the importance of choosing an appropriate OMI value in optimizing the system performance.

In Fig. 4, we plot the derived average BEP given by (23) versus the received optical power for different types of modulation, i.e., QPSK, 16-QAM, and 64-QAM, and different values of scintillation parameters α, β, i.e., $(\alpha, \beta) = \{(4,1), (4,4)\}$ with the total OMI $m_{\text{Total}} = 10\%$. The effect of the atmospheric turbulence on the received BEP is clearly apparent. The performance of the system is drastically degraded when the scintillation index is high. However, for the BEP $= 10^{-2}$, the QPSK without turbulence outperforms QPSK with $(\alpha, \beta) = (4,4)$ and QPSK with $(\alpha, \beta) = (4,1)$ by approximately 5 dB and 15 dB, respectively. Furthermore, when the received optical power $P_{r,0} = -15$ dBm, for example, the BEP increases from 7×10^{-6} at $(\alpha, \beta) = (4,4)$ to 8×10^{-3} at $(\alpha, \beta) = (4,1)$ for QPSK and from 6×10^{-4} at $(\alpha, \beta) = (4,4)$ to 2×10^{-2} at $(\alpha, \beta) = (4,1)$ for 64-QAM. In fact, the larger constellation sizes require higher received power to accurately discriminate among the transmitted symbols; they are also more sensitive to the heavy turbulence due to the required precision in accurate constellation scaling at the receiver.

Next, we analyze the system's outage probability using the equation given by (27). Fig. 5 shows the average outage probability in terms of the received optical power in dBm for different values of scintillation parameters α, β, i.e., $(\alpha, \beta) = \{(4,1), (4,4)\}$ and $m_{\text{Total}} = 10\%$. Two cases of CNDR threshold level have been considered: $\text{CNDR}_{\text{th}} = \{10 \text{ dB}, 30 \text{ dB}\}$. Similar to the BEP, It is observed that the system outage probability is severely affected by the atmospheric turbulence and requires higher received power to overcome the performance degradation. For the received optical power $P_{r,0} = -10$ dBm, for example, the outage probability increases from 2×10^{-5} to 2×10^{-2} and from 2×10^{-2} to close to 2×10^{-1} for the $\text{CNDR}_{\text{th}} = 10$ dB and $\text{CNDR}_{\text{th}} = 30$ dB, respectively. It should be noted that this result is given for a fixed value of the OMI $m_{\text{Total}} = 10\%$, which is not optimal for all the values of the received power as mentioned earlier (see Fig. 3).

To highlight the fundamental role of the optimal OMI for the overall system performance, Fig. 6, plots the optimal outage probability in terms of the received optical power $P_{r,0}$ and total optimal OMI

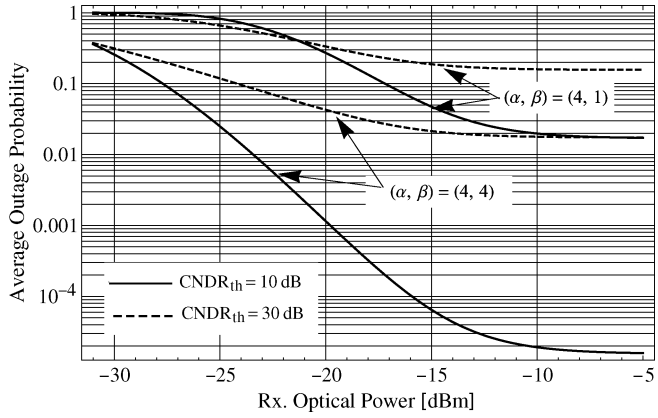

Fig. 5. Variation of the outage probability versus the received optical power.

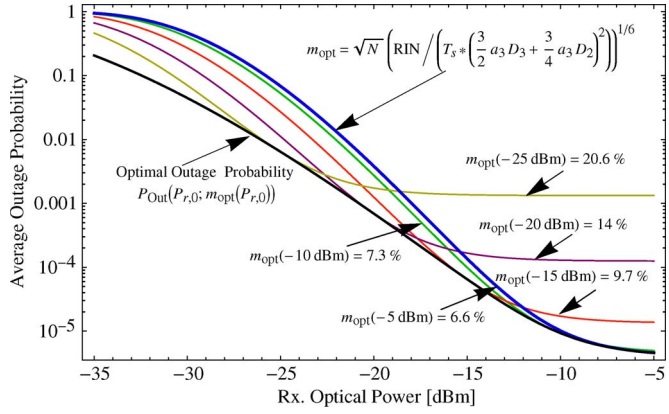

Fig. 6. Variation of the average outage probability with the received optical power for different values of OMI.

m_{opt} with scintillation parameters $(\alpha, \beta) = (4, 4)$ and $\text{CNDR}_{\text{th}} = 10$ dB. In the graph, the optimal outage probability $P_{\text{Out}}(P_{r,0}; m)$ is derived by substituting (17) into (27), and then, for each value of the received optical power, the optimal OMI m_{opt} is selected in order to minimize the outage as $P_{\text{Out}}(P_{r,0}; m) = P_{\text{Out}}(P_{r,0}; m_{\text{opt}}(P_{r,0}))$. Note that $P_{\text{Out}}(P_{r,0}; m_{\text{opt}}(P_{r,0}))$ can be seen as a lower bound of the whole system outage probability, which is difficult to achieve. We also plotted the outage probability $P_{\text{Out}}(P_{r,0}; m_{\text{opt}}(P^*_{r,0}))$ for different values of the m_{opt} selected for a specified value of received optical power $P^*_{r,0} = \{-25\ \text{dBm}, -20\ \text{dBm}, -15\ \text{dBm}, -10\ \text{dBm}, -5\ \text{dBm}\}$, and thus, by using (17), the optimal OMI $m_{\text{opt}}(P^*_{r,0})$ can be obtained as $m_{\text{opt}}(P^*_{r,0}) = \{6.6\%, 7.3\%, 9.7\%, 14\%, 20.6\%\}$. Furthermore, from (17), it can be derived that $m_{\text{opt}}(P_{r,0}) \longrightarrow \sqrt{N} \times [\text{RIN}/(T_s * ((3/2)a_3 D_3 + (3/4)a_3 D_2)^2)]^{1/6}$ when $P_{r,0}$ is high, which may be considered as upper bound of the outage probability $P_{\text{Out}}(P_{r,0}; m_{\text{opt}}(P^*_{r,0}))$. By observing Fig. 6, we notice that the value of the outage clearly depends on the optimal OMI m_{opt} for different levels of the received optical power $P_{r,0}$. Moreover, if we set the OMI to $m_{\text{opt}}(P^*_{r,0})$, the $P_{\text{Out}}(P_{r,0}; m_{\text{opt}}(P^*_{r,0}))$ shows a constant behavior due to the nonlinear distortion when $P_{r,0} > P^*_{r,0}$, and the outage penalty in comparison with $P_{\text{Out}}(P_{r,0}; m_{\text{opt}}(P_{r,0}))$ increases with the decrease of the value of $P^*_{r,0}$. However, when $P_{r,0} < P^*_{r,0}$, the outage penalty in comparison with $P_{\text{Out}}(P_{r,0}; m_{\text{opt}}(P_{r,0}))$ increases with the increase of the power $P^*_{r,0}$. These results indicate that the optimal OMI $m_{\text{opt}}(P^*_{r,0})$ should be selected so that the area between its corresponding outage $P_{\text{Out}}(P_{r,0}; m_{\text{opt}}(P^*_{r,0}))$ and the optimal outage probability $P_{\text{Out}}(P_{r,0}; m_{\text{opt}}(P_{r,0}))$ is minimal (i.e., $\text{Min}_{P^*_{r,0}}\{|\int (P_{\text{Out}}(P_{r,0}; m_{\text{opt}}(P^*_{r,0})) - P_{\text{Out}}(P_{r,0}; m_{\text{opt}}(P_{r,0}))) dP_{r,0}|\}$).

4. Conclusion

In this paper, we have studied the transmission performance of the OFDM signals over a turbulent RoFSO channel in terms of the average CNDR, BEP, and outage probability. We have presented a mathematical model for the optimization of the OFDM-RoFSO link and closed-form expressions for the system BEP and outage probability, taking into account the optical noises and the nonlinear distortion effects of the IM/DD MSM optical link. The FSO channel turbulence-induced fading is modeled by gamma–gamma distribution, which covers the weak to strong turbulence regime. In contrast to the optical fiber communication, our results demonstrated that the RoFSO system performance is highly sensitive to the atmospheric turbulence and the received optical power. However, it has shown that selecting an appropriate optimal optical modulation index may increase the overall system performance.

References

[1] H. Willebrand and B. Ghuman, *Free Space Optics: Enabling Optical Connectivity in Today's Networks*. London, U.K.: Sams, 2002.
[2] V. W. S. Chan, "Free-space optical communications," *J. Lightwave Technol.*, vol. 24, no. 12, pp. 4750–4762, Dec. 2006.
[3] H. Al-Raweshidy and S. Komaki, Eds., *Radio Over Fiber Technologies for Mobile Communications Networks,* 1st ed. Norwell, MA: Artech House, 2002.
[4] K. Kazaura, K. Wakamori, M. Matsumoto, T. Higashino, K. Tsukamoto, and S. Komaki, "RoFSO: A universal platform for convergence of fiber and free-space optical communication networks," *IEEE Commun. Mag.*, vol. 48, no. 2, pp. 130–137, Feb. 2010.
[5] K. Tsukamoto, K. Nakaduka, M. Kamei, T. Higashino, S. Komaki, K. Wakamori, Y. Aburakawa, T. Nakamura, K. Takahashi, T. Suzuki, K. Kazaura, K. Ohmae, M. Matsumoto, S. Kuwano, and H. Watanabe, "Development of DWDM Radio on free space optic link system for ubiquitous wireless," in *Proc. AP-MWP Conf.*, Apr. 2007, pp. 295–296.
[6] D. Kedar and S. Arnon, "Urban optical wireless communication networks: The main challenges and possible solutions," *IEEE Commun. Mag.*, vol. 42, no. 5, pp. S2–S7, May 2004.
[7] K. Tsukamoto, A. Hashimoto, Y. Aburakawa, and M. Matsumoto, "The case for free space," *IEEE Microw. Mag.*, vol. 10, no. 5, pp. 84–92, Aug. 2009.
[8] A. Bekkali, P. T. Dat, K. Kazaura, K. Wakamori, M. Matsumoto, T. Higashino, K. Tsukamoto, and S. Komaki, "Performance evaluation of an advanced DWDM RoFSO system for transmitting multiple RF signals," *IEICE Trans. Fundam. Electron. Commun. Comput. Sci.*, vol. E92-A, no. 11, pp. 2697–2705, Nov. 2009.
[9] R. V. Nee and R. Prasad, *OFDM for Wireless Multimedia Communications*. Norwell, MA: Artech House, 2000.
[10] R. Hui, B. Zhu, R. Huang, C. T. Allen, K. R. Demarest, and D. Richards, "Subcarrier multiplexing for high-speed optical transmission," *J. Lightwave Technol.*, vol. 20, no. 3, pp. 417–427, Mar. 2002.
[11] J. M. Cioffi, "A multicarrier primer," in *ANSI Contribution T1E1*, Nov. 1991, pp. 4/91–157.
[12] J. Armstrong, "OFDM for optical communications," *J. Lightwave Technol.*, vol. 27, no. 3, pp. 189–204, Feb. 2009.
[13] J. Armstrong and A. J. Lowery, "Power efficient optical OFDM," *Electron. Lett.*, vol. 42, no. 6, pp. 370–372, Mar. 2006.
[14] P. Horvath and I. Frigyes, "Effects of the nonlinearity of a Mach-Zehnder modulator on OFDM radio-over-fiber transmission," *IEEE Commun. Lett.*, vol. 9, no. 10, pp. 921–923, Oct. 2005.
[15] L. Chen, B. Krongold, and J. Evans, "Performance evaluation of optical OFDM systems with nonlinear clipping distortion," in *Proc. IEEE ICC*, 2009, pp. 1–5.
[16] R. W. Bauml, R. F. H. Fischer, and J. B. Huber, "Reducing the peak-to-average power ratio of multicarrier modulation by selected mapping," *Electron. Lett.*, vol. 32, no. 22, pp. 2056–2057, Oct. 1996.
[17] J. Armstrong, "Peak-to-average power reduction for OFDM by repeated clipping and frequency domain filtering," *Electron. Lett.*, vol. 38, no. 5, pp. 246–247, Feb. 2002.
[18] L. C. Andrews and R. L. Phillips, *Laser Beam Propagation Through Random Media*, 2nd ed. Bellingham, WA: SPIE, 2005.
[19] J. Proakis, *Digital Communications*, 4th ed. New York: McGraw-Hill, 2001.
[20] Wolfram Function Site, 2010. [Online]. Available: http://functions.wolfram.com/
[21] I. S. Gradshteyn and I. M. Ryzhik, *Table of Integrals, Series, and Products,* 5th ed. London, U.K.: Academic, 1994.
[22] *Transmission System for Digital Terrestrial Television Broadcasting*, ARIB STD-B31, (accessed on April 2010). [Online]. Available: http://www.arib.or.jp/english/html/overview/ov/std_b31.html